Diamond & Related Materials 17 (2008) 967–971

Contents lists available at ScienceDirect

Diamond & Related Materials

journal homepage: www.elsevier.com/locate/diamond

Humidity effect on friction behaviors of nano-undulated diamond-like carbon films

Jin Woo Yi [a,b], Se Jun Park [a], Myoung-Woon Moon [a,*], Kwang-Ryeol Lee [a], Seock-Sam Kim [b]

[a] Future Fusion Technology Laboratory, Korea Institute of Science and Technology, Seoul 130-650, South Korea
[b] School of Mechanical Engineering, Kyungpook National University, Daegu 702-701, South Korea

ARTICLE INFO

Article history:
Received 20 August 2007
Received in revised form 7 November 2007
Accepted 22 February 2008
Available online 6 March 2008

Keywords:
Diamond-like carbon
Nano-patterns
Ni dot
Relative humidity
Tribology

ABSTRACT

Humidity dependency of friction behavior of nano-undulated diamond-like carbon (DLC) films was investigated by a home-made ball-on-disk type tribometer under controlled relative humidity of 0, 50, and 90%. Nano-undulated DLC films with surface roughness ranging from 0.2 to 13.4 nm were prepared by deposition of DLC film on the Si substrate with Ni nanodots. Friction coefficient of the flat DLC surface increased with the relative humidity, while that of the nano-undulated surfaces revealed smaller dependence on the relative humidity. When the surface roughness increased to 13.4 nm, friction behavior was observed to be independent of the relative humidity. The analysis of chemical composition and atomic bond structure of the debris and the transfer layer revealed that the humidity dependence on the nano-undulated surface was minimized by suppressing the graphitization of the transfer layer even with high concentration of Fe in the debris.

1. Introduction

Diamond-like carbons (DLC) films have been considered as a strong candidate for a protective layer on the medical implant materials such as artificial hip or knee joint. DLC surface is atomically smooth and biocompatible with low friction coefficient, strong resistance against wear particle formation, and excellent mechanical properties of high elastic modulus and hardness [1–7]. The friction coefficient of the DLC film against steel ball has been reported to be about 0.1 under high vacuum and dry condition, or much less with modification of microstructures or chemical composition [9–12]. However, application of DLC film is limited due to its sensitivity to the environmental conditions, especially relative humidity (RH) [8]. The friction coefficient could rise up to 0.6 under highly humid or oxygen environment [13–16]. Various theories have been proposed to explain the environmental dependence of the frictional behavior of DLC film [17–19]. The friction and wear mechanism of DLC film is yet to be sufficient to explain the role of the environment on the tribological behavior of DLC film.

The surface roughness has been also considered as one of the key parameters to affect the tribological behavior of a wear protecting thin film such as TiN, WC/C [20] and DLC film [21]. In macro-scale tribology, it was reported that the surface roughness could reduce the friction coefficient by suppressing the wear particle generation, removing the wear particle from sliding interface and preventing the agglomeration of wear particles [22,23]. Recently Park et al. [21] have investigated the frictional behaviors of the DLC films with the surface roughness in nanometer scale. They reported that the nano-undulated surface could suppress the tribo-chemical reaction between the film surface, the counter-face ball, and environment, resulting in the minimum friction coefficient in ambient air.

In the present work, we focused on the humidity dependence of the friction behavior of the DLC films with nano-undulated surface. Surface roughness of the nano-undulated surface was varied in the range from 3.0 to 13.4 nm in root mean square (RMS) value. The nano-undulated surfaces were prepared by DLC film deposition on the Si substrate with Ni nano-dots of diameters ranging from 81 to 540 nm (Fig. 1). Friction and wear behaviors were explored with measurement of friction coefficient during tribo-test (Figs. 2–4) and observation on the wear track and counter ball surface using microscopic and chemical analysis (Figs. 5–7). Experimental details for fabrication of the nano-undulated DLC films and tribo-test under controlled humidity environment were provided as below.

2. Experimental

2.1. DLC film coated on nanopatterns

DLC films were deposited on nano-sized Ni dots fabricated on Si substrate by annealing Ni thin film. The Ni thin film was deposited on 600-μm-thick Si (100) wafer by DC magnetron sputtering at the power of 40 W (Fig. 1a). The Ni thin film of thickness ranging from 3 to 18 nm changed into nano-sized Ni dots by annealing the specimen in a rapid thermal process furnace at 800 °C for 10 min in pure hydrogen environment [24]. Ni dots of diameter ranging from 81 to 540 nm were fabricated depending on the Ni thin film thickness (Fig. 1b). DLC films were then deposited by a radio-frequency plasma assisted chemical vapor deposition (r.f.-PACVD) using methane as the precursor gas (Fig. 1c). Details of the DLC deposition condition were

* Corresponding author.
E-mail address: mwmoon@kist.re.kr (M.-W. Moon).

0925-9635/$ – see front matter © 2008 Elsevier B.V. All rights reserved.
doi:10.1016/j.diamond.2008.02.041

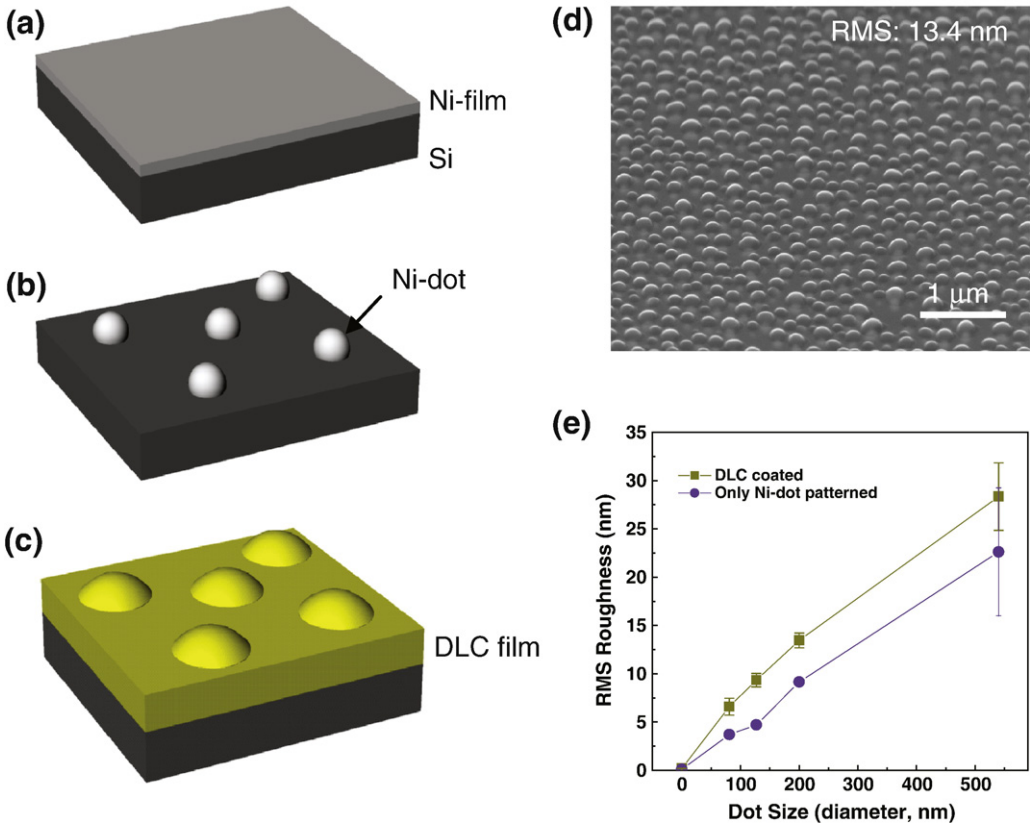

Fig. 1. Procedures for DLC coatings on nano-patterned Si substrate. (a) Deposition of Ni thin film on Si using DC magnetron sputtering, (b) Ni nano-dot formation using thermal annealing at 800 °C using RTP system, and (c) DLC film coating on nano-patterned surface with PE-CVD method. (d) SEM images of DLC coating on Ni-dot nano-patterned surface with the roughness of 13.44 nm in RMS scale. (e) Graph of the surface roughness for the surfaces of Ni dot patterned substrate with (rectangle) and without (circle) DLC film coating, AFM scanning area was 2×2 μm^2 for all cases.

described elsewhere [21]. 100 nm thick DLC films were deposited on the Si wafer with Ni nanosized dots at the negative bias voltage −150 V and deposition pressure 1.33 Pa.

Fig. 1d showed the SEM microstructure of the nano-undulated DLC surface prepared in the present work. Roughness of the Ni dot patterned surfaces with and without DLC film was linearly dependent on the Ni dot size as shown in Fig. 1e. Roughness for a DLC film deposited on flat Si substrate was estimated to be about 0.19 nm in the root mean square (RMS) roughness, similar to the value for a bare Si substrate [21]. As the size of Ni dots increased, RMS roughness increased from 3.7 to 22.6 nm before deposition of DLC films. With DLC film on the Ni dot patterned surface, the roughness increased from 6.6 to 28.4 nm.

2.2. Tribology test under humidity condition

Friction and wear behaviors were investigated by using a home-made ball-on-disc type wear rig installed inside an environmental chamber depicted in Fig. 2. The steel bearing ball (AISI 52100) of 6-mm diameter was set for sliding over the DLC surface with a sliding speed at 11.6 cm s^{-1} and a normal load of 2 N. The tangential force was measured by a load cell of 9.8 N in full scale. The number of cycle of tribology test was fixed at 10,000 corresponding to the total sliding distance of 314.2 m. The tribo-tests were performed at room temperature with three values of relative humidity (RH); 0, 50, and 90%. RH value was controlled in the range of ±2.5% by using a humidity controller attached to the tribo-chamber.

2.3. Analysis

Surface morphology of nano-undulated DLC surfaces was observed using atomic force microscopy (AFM, Hysitron Inc.) and scanning electron microscopy (SEM, NanoSEM, FEI company) before and after tribo-test. Micro-Raman spectroscopy (LabRam HR, Jobin-Yvon) was adopted for the analysis of atomic bond structure of the transfer layer on the steel ball surfaces. Chemical composition of the wear debris formed between DLC surface and steel ball was measured by an Auger

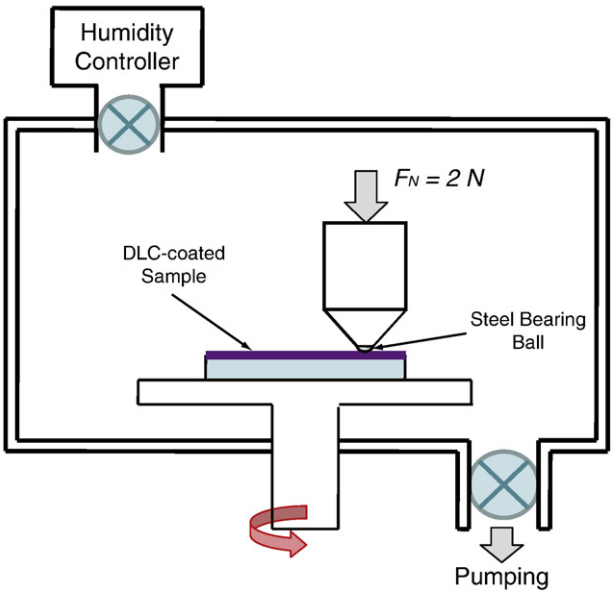

Fig. 2. A schematic figure for the tribo-test system equipped with a humidity controller controlling the relative humidity during test.

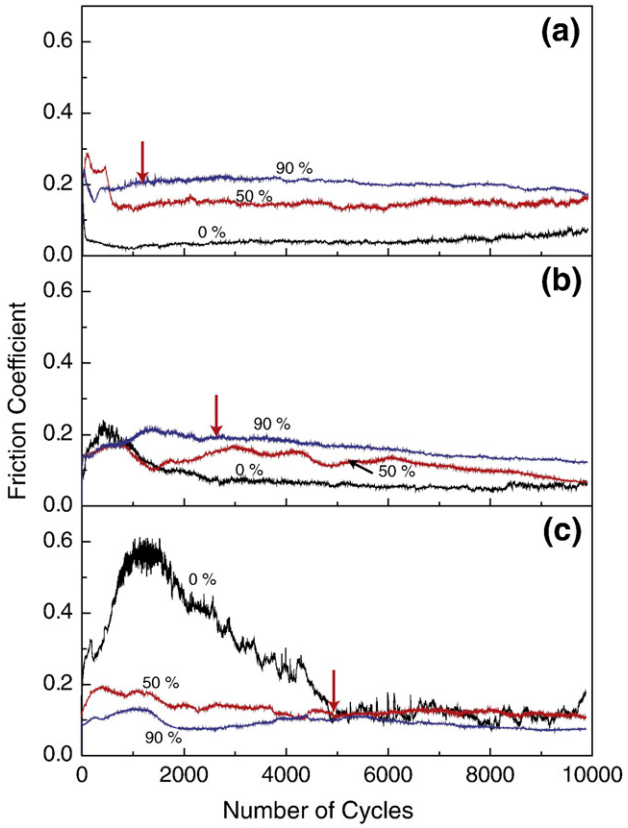

Fig. 3. The variation of the friction coefficient with three selected pattern sizes under controlled RH value of 0, 50, and 90%. RMS roughness was measured on flat DLC film with 0.2 nm (a), and nano-undulated DLC film with 6.6 nm (b), and 13.4 nm (c). Red arrows indicated a transition point where frictional behaviors changes from unstable to stable. (For interpretation of the references to colour in this figure legend, the reader is referred to the web version of this article.)

electron spectroscopy (AES, MODEL 670, PHI Inc.). Before AES analysis, the specimen surface was cleaned by Ar ion beam sputtering for 1 min and the spectra were normalized with respect to the oxygen peak value.

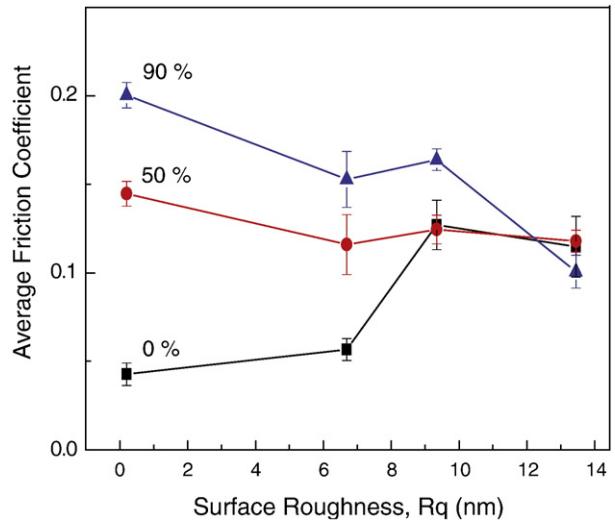

Fig. 4. Average friction coefficients with increase of surface roughness of nano-undulated Ni nano-patterns under controlled condition of RH 0, 50, and 90%.

3. Results and discussion

3.1. Friction coefficient under humidity environment

Fig. 3 shows the evolution of the friction behaviors for various values of the relative humidity. For DLC films with flat surface or RMS roughness of 0.19 nm (Fig. 3a), the friction coefficient increased from a value lower than 0.05 in dry condition to 0.21 when RH was 90%. This is a typical humidity dependence of the friction behavior previously reported in the literatures [8,19,25]. In contrary, as the surface roughness increased, the humidity dependence of the friction became less significant and eventually disappeared when the surface roughness was 13.4 nm. In dry condition of 0% RH, the initial run-in regime of the friction coefficient was observed before 5000 cycles on the nano-undulated DLC films (See Fig. 3b and c). The initial run-in was more significant with increasing surface roughness in dry condition. However the initial run-in regime got shorter and disappeared as the RH value increased in both cases of the surface roughness, 6.6 (Fig. 3b) and 13.4 nm (Fig. 3c).

Fig. 4 shows the friction coefficient averaged over the stable regime of Fig. 3. In dry air condition, the friction coefficient increased from 0.05 to 0.13 as the surface roughness increased from 0.2 to 13.4 nm. This increase is presumably due to the increase in the contact pressure on the

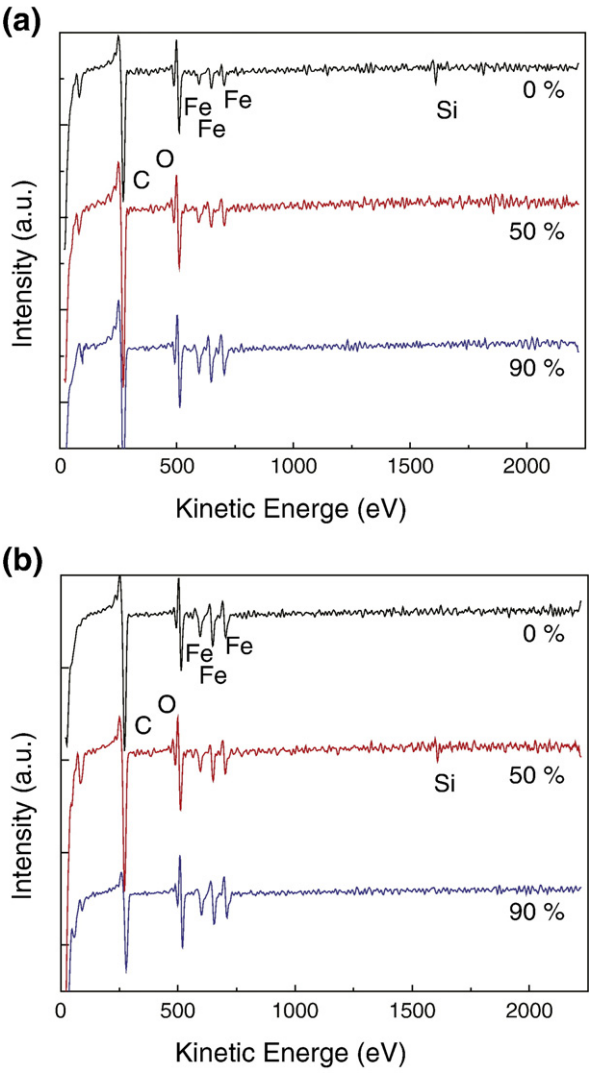

Fig. 5. Wear debris was examined using AES for two cases of DLC surface with RMS 0.2 nm (or flat surface) (a) and 13.4 nm (b) as changed humidity with 0, 50, and 90%.

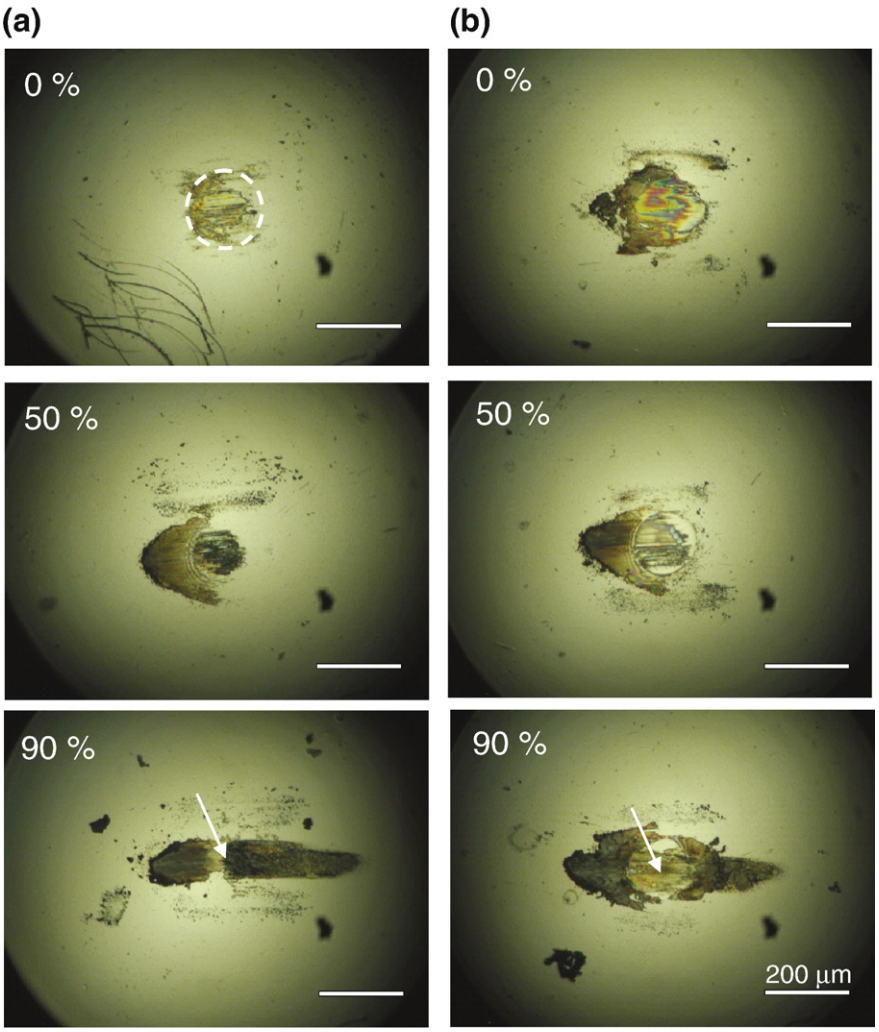

Fig. 6. Optical microscopic images on the steel ball surfaces contacting to different surfaces of the flat (RMS roughness = 0.2 nm) (a) and nano-undulated (RMS = 13.4 nm) (b) DLC films with respect to 0, 50 and 90% RH.

rough surface, which would enhance the plastic deformation of the contacting materials. However, in the humid environment of 50 and 90% RH, the friction coefficient gradually decreased with the surface roughness. It is also evident from Fig. 4 that the increase in the surface roughness of DLC film in nanometer scale minimizes the humidity dependence of the friction coefficient.

3.2. Analysis of chemical reaction on contacting areas

To explore the humidity dependence of the friction behavior of the nano-undulated surfaces the chemical components of the debris accumulated in the vicinity of the wear track was characterized by Auger spectroscopy. On the flat DLC surface, the concentration of Fe composition contained in the wear debris increased with RH values as shown in Fig. 5a, indicating that the wear rate of the steel ball was enhanced in high humid environment. In previous work [25,26], it was suggested that the increased value in friction coefficient for flat DLC films is strongly related to the enriched Fe in the wear debris, since the Fe-rich debris causes high and unstable friction behavior similar to those in Fig. 3a. However, on the nano-undulated DLC surfaces of RMS roughness 13.44 nm, the concentration of the Fe did not change with the RH value as shown in Fig. 5b. It is worthwhile noting that the friction coefficient was also invariant with the humidity on the nano-undulated surface of RMS roughness 13.4 nm (see Fig. 4). This result implies that the humidity dependence of the friction behavior is closely related to that of Fe concentration in the debris.

Fig. 6 shows the optical microstructure of the transfer layer formed on the wear scar of the counter-face steel ball. In general, diameter of the wear scar was smaller when sliding against the flat DLC surface. In this case, transferred materials form a layer which seems to be thicker in more humid environment as indicated by an arrow in Fig. 6a. In the case of the nano-undulated DLC surface of RMS roughness 13.4 nm, thin transfer layer was found on the relatively large wear scar (see an arrow in Fig. 6b). In contrast to the case of flat DLC surface, the morphology of the transfer layer is similar regardless of the RH values.

Atomic bond structure of the transfer layer was examined using a micro-Raman spectroscope. Fig. 7a shows the Raman spectra of the transfer layer after sliding against the flat DLC surface for various humidity conditions. In dry environment, the Raman spectrum reveals that the transfer is the graphitic carbon that is characterized by well separated D (1320 cm^{-1}) and G peaks (1530 cm^{-1}). As the humidity increased, the carbon peak changed to an irregular shape. However, it is obvious from the Raman spectra that the graphitization of the transfer layer occurred even in high humid environment (see the spectra of pure DLC film). The Raman spectrum analysis suggests that the tribo-chemical reaction during sliding against the flat surface is so significant that the conversion of the transfer layer to graphitic phase occurred even under high humidity environment. As reported in the literatures [27–30], the graphitization of the debris or the transfer layer would enhance the humidity dependence of the friction and wear behaviors. At high sliding speed, the tribo-chemical reaction would be further accelerated by the high temperature of the contacting area [21,25,1,25].

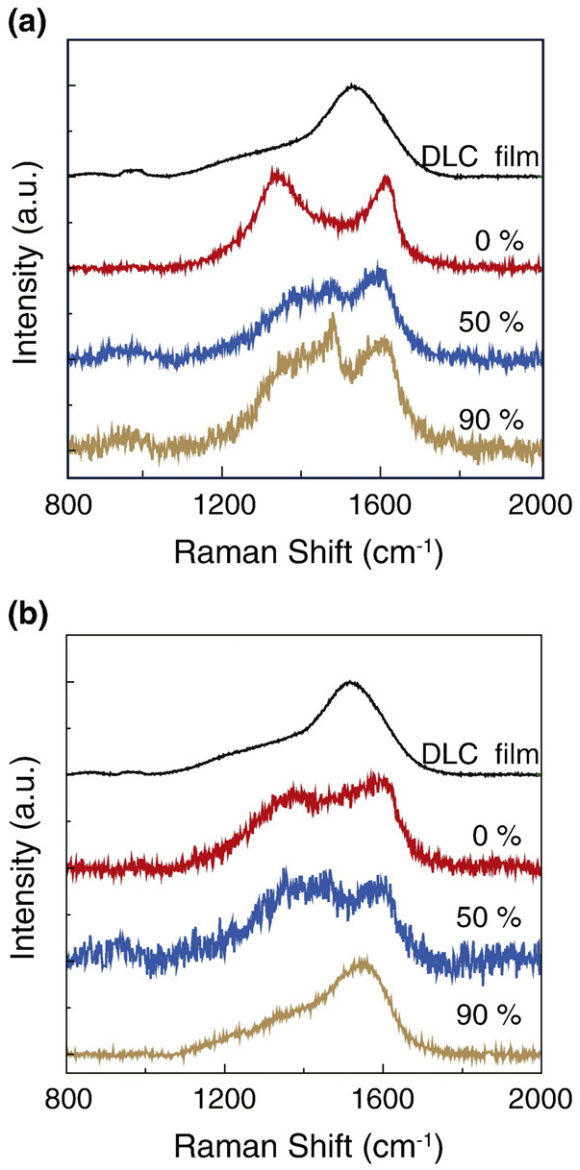

Fig. 7. Raman spectroscopy used for the examination of chemical compositions on the steel ball surface slid over the two different undulated DLC surfaces with RMS of 0.2 nm (flat) (a) and 13.4 nm (b) under 0, 50, and 90% RH. The spectra for pure DLC film with G-peak of 1532 cm^{-1} was compared to those for each condition.

Fig. 7b is the Raman spectra of the transfer layer on the wear scar after sliding against the nano-undulated surface of RMS roughness 13.4 nm. The carbon Raman peak shows that the transfer layer was converted to the graphitic materials, whereas the tribo-chemical reaction was suppressed with increasing relative humidity. One should note that the transfer layer remains as diamond-like when sliding under the humid environment of relative humidity, 90%. This result shows that no significant change of graphitic materials are involved in the contacting area under high humid environment of relative humidity 90%. The Fe-rich wear debris seems to be removed from the contacting interface as a steel ball slides over the nano-undulated surface. The tribo-chemical reaction such as oxidation and graphitization of carbon [31] would be thus less significant on the nano-undulated surface, resulting in the minimization of the humidity dependence of the friction behavior as shown in Fig. 4.

4. Conclusions

The most important observation of the present work is that a nano-undulated DLC surface minimizes the humidity dependency of the friction behavior by suppressing the tribo-chemical reaction between the steel ball and the DLC film. The humidity dependence of the friction was not observed on the nano-undulated DLC surface, while the friction coefficient on the flat DLC surface increased with relative humidity of the test environment. Fe concentration in the debris on the nano-undulated surface was constant irrespective with the relative humidity. Furthermore at 90% RH, Fe rich debris seems to be continuously removed from the contacting area during sliding against the nano-undulated surface. Hence, the DLC-like bond structure of the transfer layer on the wear scar on steel ball surface showed almost no change while the transfer layer on the wear scar was graphitic when sliding on the flat surface.

Acknowledgements

This work was financially supported by part from a grant (code #: 05 K1501-01610) by 'Center for Nanostructured Materials Technology' under '21st Century Frontier R&D Programs' of the Ministry of Science and Technology, Korea. JWY and SSK acknowledge the financial support from Kyungpook National University.

References

[1] A.C. Evans, J. Franks, P.J. Revell, Surf. Coat. Technol. 47 (1991) 662.
[2] L.A. Thomson, F.C. Law, N. Rushton, J. Franks, Biomaterials 12 (1991) 37.
[3] C. Du, X.W. Su, F.Z. Cui, X.D. Zhu, Biomaterials 19 (1998) 651.
[4] M. Allen, B. Myer, N. Rushton, J. Biomed. Mater. Res. 58 (2001) 319.
[5] V. Saikko, T. Ahlroos, O. Calonius, J. Keranen, Biomaterials 22 (2001) 1507.
[6] V.M. Tiainen, Diamond Relat. Mater. 10 (2001) 153.
[7] A.D. Reisel, C. Schurer, E. Muller, Diamond Relat. Mater. 13 (2004) 823.
[8] R. Gilmore, R. Hauert, Surf. Coat. Technol. 133–134 (2000) 437.
[9] C. Donnet, Surf. Coat. Technol. 100–101 (1998) 180.
[10] A.A. Voevodin, J.M. Schneider, C. Rebholz, A. Matthews, Tribol. Int. 29 (7) (1996) 559.
[11] K. Miyoshi, B. Pohlchuck, K.W. Street, J.S. Zabinski, J.H. Sanders, A.A. Voevodin, R.L.C. Wu, Wear 225–229 (1999) 65.
[12] J.A. Heimberg, K.J. Wahl, I.L. Singer, A. Erdemir, Appl. Phys. Lett. 78 (17) (2001) 2449.
[13] K. Enke, Thin Solid Films 80 (1981) 227.
[14] R. Memming, H.J. Tolle, P.E. Wierenga, Thin Solid Films 143 (1986) 31.
[15] A.K. Gangopadhyay, W.C. Vassell, M.A. Tamor, P.A. Willermet, J. Tribol. 116 (1994) 454.
[16] B. Marchon, N. Heiman, M.R. Khan, IEEE Trans. Magn. 26 (1) (1990) 168.
[17] C. Donnet, M. Belin, J.C. Auge, J.M. Marin, A. Grill, V. Patel, Surf. Coat. Technol. 68–69 (1994) 626.
[18] Y. Liu, A. Erdemir, E.I. Meletis, Surf. Coat. Technol. 94–95 (1997) 463.
[19] S.J. Park, J.-K. Kim, K.-R. Lee, D.-H. Ko, Diamond Relat. Mater. 12 (2003) 1517.
[20] P. Harlin, P. Carlsson, U. Bexell, M. Olsson, Surf. Coat. Technol. 201 (2006) 4253.
[21] S.-J. Park, K.-R. Lee, D.-H. Ko, Diamond Relat. Mater. 14 (2005) 1291.
[22] S.T. Oktay, N.P. Suh, J. Tribol. 114 (1992) 378.
[23] N.P. Suh, M. Mosleh, P.S. Howard, Wear 175 (1994) 151.
[24] C.S. Lee, T.-Y. Kim, K.-R. Lee, J.-P. Ahn, K.H. Yoon, Chem. Phys. Lett. 380 (2003) 774.
[25] S.J. Park, K.-R. Lee, D.-H. Ko, Tribol. Int. 37 (2004) 913.
[26] D.S. Kim, T.E. Fischer, B. Gallois, Surf. Coat. Technol. 49 (1991) 537.
[27] A.A. Voevodin, A.W. Phelps, J.S. Zabinski, M.S. Donley, Diamond Relat. Mater. 5 (1996) 1264.
[28] J.P. Hirvonen, R. Lappalainen, J. Koskinen, A. Anttila, T.R. Jervis, M. Trkula, J. Mater. Res. 5 (11) (1990) 2524.
[29] K. Jia, Y.Q. Li, T.E. Fischer, B. Gallois, J. Mater. Res. 10 (6) (1995) 1403.
[30] Y. Liu, A. Erdemir, E.I. Meletis, Surf. Coat. Technol. 82 (1996) 48.
[31] J. Fujita, M. Ishida, T. Ichihashi, Y. Ochiai, J. Vac. Sci. Technol., B 20 (2002) 2686.